Proceedings of 2023 IEEE
International Conference on Mechatronics and Automation
August 6 - 9, Harbin, Heilongjiang, China

Design and Characteristic Evaluation of a Novel Clamping Mechanism for Amphibious Spherical Bionic Robots

Chengchao Gu[1], Shuxiang Guo[1, 2*], Meng Liu[1], He Yin[1], Ao Li[1]

[1] Key Laboratory of Convergence Medical Engineering System and Healthcare Technology, the Ministry of Industry and Information Technology, School of Life Science, Beijing Institute of Technology, No.5, Zhongguancun South Street, Haidian District, Beijing 100081, China.

[2] The Department of Electronic and Electrical Engineering, Southern University of Science and Technology, Shenzhen, Guangdong 518055, China.

{ gucc & guoshuxiang } @bit.edu.cn;

** Corresponding author*

***Abstract* - The motion function and control of amphibious robots is a hot topic at present. The multi-function of robot is the development trend of robot. In this paper, based on the existing prototype bionic robot in the laboratory, the structure of the robot's mechanical leg is updated, and the underwater grasping function is successfully added. The new mechanical leg integrates a mechanical claw device, which makes use of the geometric characteristics of the parallelogram to shrink the mechanical claw, maximizes the use of the limited space below the robot, and greatly extends the effective length of the grasping end of the mechanical claw. At the same time, through static stress analysis and motion simulation, the designed structure was evaluated and analyzed, and the appropriate servo specifications and structure size were obtained, which verified that the current designed structure can complete the grasping task of 3kg objects. Finally, 3D printing technology was used to complete the production of the first version of the new mechanical leg, and the functional verification experiment of grasping objects of two different sizes was completed by using the steering gear control.**

Index Terms – integration, mechanical gripper, contractible, simulated analysis, functional verification experiment

I. INTRODUCTION

Influenced by amphibians in nature, researchers have gradually shifted the research direction of robots to the design and manufacture of bionic amphibious robots inspired by amphibian biological structures [1]. The amphibious concept of amphibious robots is generally considered to be in both land and underwater environments, including coastal and swampy environments. Robots that are capable of accomplishing related tasks in amphibious environments using a mixture of multiple sensors [2] are considered of great practical significance, such as ocean exploration, search and rescue, Marine environmental protection, military reconnaissance, etc. [3]. About the development direction of amphibious robot, there are roughly the following bionic objects: crab, snake, turtle, shrimp, lizard, frog, crocodile, etc. [4]. Meanwhile, the current development of amphibious robots only considers the motion strategy and control of existing robots in the land and underwater environment [5-7], controls the cooperative operation and formation of multiple robots [8-11], and seeks more ways to communicate among multiple robots [12,13]. Or consider using different materials to build robots [14,15].

Fig. 1 shows some bionic prototypes and related robots [16,17]. In October 2022, the adaptive bionic turtle developed by the Yale University team was the most effective amphibious robot achievement recently [17], and the poster of its research results became the cover of Nature magazine.

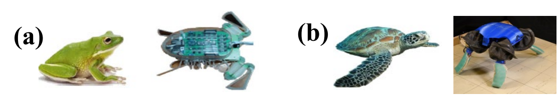

Fig. 1 The bionic prototype and the associated robot: (a) The frog robot [16]; (b) The turtle robot [17]

In addition to general mobility, locomotion capabilities, some other operational capabilities are expected to be added to the robot. In the underwater environment, grasping objects is a very common application scenario. However, in the current development of underwater manipulators, the structure of the manipulator is often large in overall volume. A manipulator simulating a human arm is used as the completion of the grasping task, and at the same time, the corresponding camera and spotlight are equipped to assist the grasping task [18]. In addition, salvage robots with grasping functions often need to first reach the destination with the robotic arm carried by the underwater vehicle, and then carry out the grasping operation, which undoubtedly greatly increases the volume of the whole robot [19-21], as shown in Fig. 2. Or a smaller manipulator is designed, but it is not integrated with the robot, and only realizes the grasping task of a single manipulator [22,23].

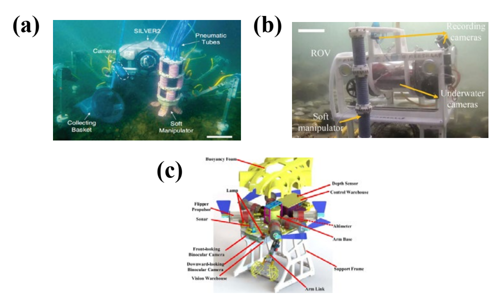

Fig. 2 Robotic arms for some underwater operations: (a) The underwater mobile manipulation [19]; (b) A soft manipulator [20]; (c) The underwater salvage robot [21]

Therefore, in view of the above development of the current amphibious bionic robot and underwater manipulator, based on the spherical amphibious robot developed by our team, this paper updates the design of the latest generation of thruster, and proposes a multifunctional mechanical leg, thruster and mechanical claw composite structure, and adds the contractile mechanical claw structure.

II. DESIGN OF A NOVEL CLAMPING MECHANISM

A. The Prototype of Novel Clamping Mechanism

First of all, the mechanical structure proposed in this design is based on the original mechanical leg structure, and the original mechanical leg is modified and extended to the mechanical claw structure. Fig. 3 is the comparison between the new structure designed in this paper and the original structure. The original mechanical structure of the robot is shown in Fig. 3(a), which adopts a three-joint and three-link mechanical leg structure corresponding to the "hip bone", “Femur” and “Tibia”. Among them, the thrusters part is fixed on the “Tibia” linkage and has 3 degrees of freedom, which is used to complete the land crawling and the water propulsion.

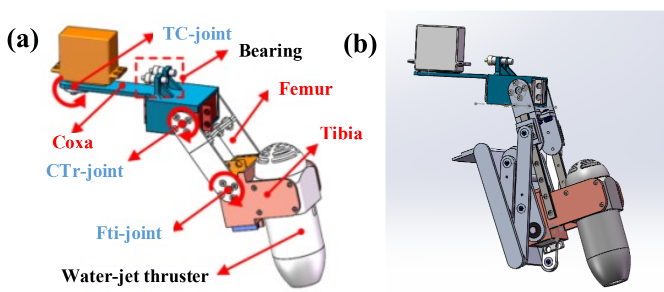

Fig. 3 The comparison of the novel structure and the original structure: (a) The original structure; (b) The novel structure

In the contraction process of the mechanical leg, it can be found that its shape is like a claw, so the leg structure is considered to expand and extend, and the claw structure is added. The “Femur” link and the “Tibia” link of the original mechanical leg structure were connected and fixed, which was defined as the new “Femur” link, and the position of the thruster was fixed on the new “Femur” link, reducing 1 degree of freedom. At the same time, the claw structure to be added is connected with the original "shin" joint, so the claw has 3 degrees of freedom, and the schematic diagram of the single-leg design and assembly complete robot is shown in Fig. 4 and Fig. 5.

B. The Novel Clamping Mechanism structure principle

To grasp an object under the robot body, a mechanical claw of a certain length is needed. However, considering the length of the leg structure and the size of the robot body, it is not enough to directly add a mechanical claw to the servo of the "shin" joint. Therefore, a mechanical claw containing a contraction structure is proposed in this paper, so that the original maximum flexible length of about 11cm is extended to about 17cm. Fig. 6 is a schematic diagram of the mechanical claw when it is open, and the four links involved in the mechanical claw are set as L_1、L_2、L_3、L_4 in this paper.

Compared with the original mechanical leg structure, the design can be divided into two parts: a. Principle of contraction; b. Principle of clamping.

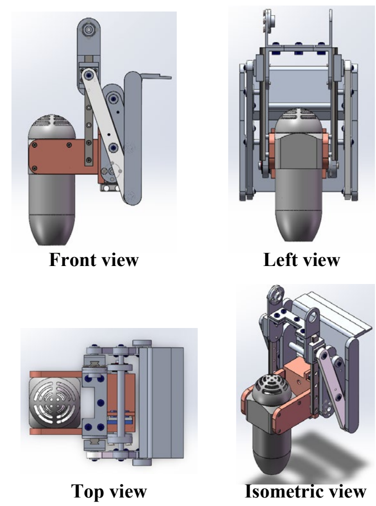

Fig. 4 Different views of the novel mechanical leg design

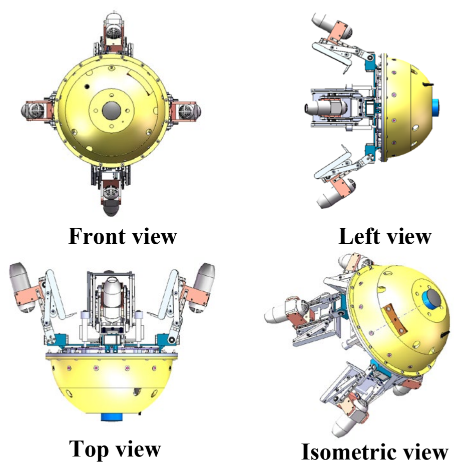

Fig. 5 Different views of novel robot

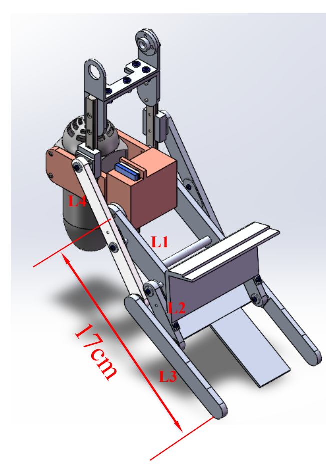

Fig. 6 The novel clawing mechanism (open state)

a. Principle of contraction

The contraction structure consists of two parts. The contraction structure mainly uses the easy deformation characteristics of the parallelogram. For the contraction process, this paper gives a simplified figure of the structure in Fig. 7. In the figure, one part is the improvement of the original "Femur" link, namely L_5. In this design, the original structure is replaced by a slider and slider structure. The endpoint e of L_4 can slide on the slider L_5. Point f is the schematic point of the steering shaft. When the servo drives, the L_1 link rotates clockwise, because the length of ed is fixed, but the endpoint d is away from L_5, so the endpoint e moves from top to bottom on L_5. At this time, L_4 rotates counterclockwise around point d, and the Angle β between L_1、L_4 increases continuously. In order to maintain the characteristics of the parallelogram, the four sides of the parallelogram $abcd$ rotate, driving the corresponding linkage structure to move, and L_3 is opened.

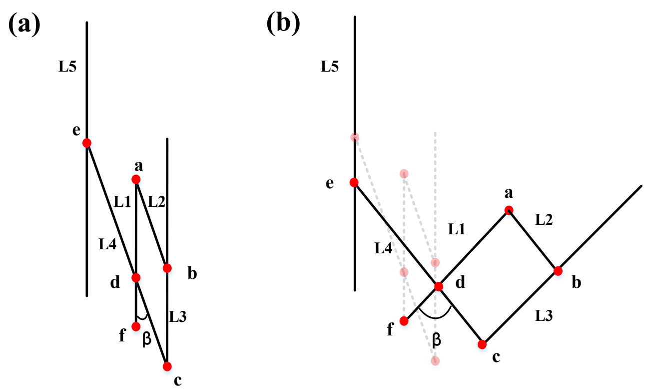

Fig. 7 The simplified structure of mechanical claw: (a) Contraction state; (b) Open state

b. Principle of clamping

In the actual clamping, considering the balance control of the robot itself, this paper proposes a pair of opposite mechanical legs to complete the clamping task, and another pair of mechanical legs is used to realize the mobile function after completing the clamping task. The closing state of the mechanical legs during clamping is shown in Fig. 8.

Among them, the mechanical claw part in addition to the contraction structure, the end of the mechanical claw uses a similar form of "three fingers", in the middle of the "finger" selected a certain width of the plate structure, while considering the relative mechanical claw in the grip of the "finger" interleaving, the middle "finger" position is set in the middle on both sides of the place.

In addition, this design considers adding a removable baffle on the L_3 link, which is used for the double clamp on both sides of the clamp. The baffle above a certain width avoids the escape of the object from above. The design of this baffle can be personalized for the object to be clamped.

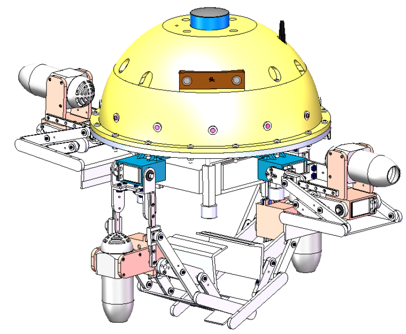

Fig. 8 The schematic of the clamping

III. SIMULATION ANALYSIS

For the proposed new structure and the addition of new functions, it is often necessary to carry out some simulation experiments [24-26], verify and optimize some common parameters, so as to improve the structure. Firstly, due to the different stress conditions of each part of the structure when the mechanical claw grasps, the static stress analysis of the structure is considered in this paper to facilitate the structural optimization design of the region with large stress. At the same time, the displacement analysis of the selected material after the stress is carried out, so as to make the optimal choice of the material. Secondly, considering that the servo at the joint position is required to provide torque to ensure the stability of the clamp, a simple kinematic simulation of the structure will be carried out in this paper, so as to determine the torque required by the servo to determine the specification of the servo. In addition, the morphology of the whole robot will change after the mechanical claw completes the grasping task underwater. Considering the possible influence of morphological changes on the ability of the robot to move in water, further underwater mobility experiments are carried out in this paper.

Regarding the use of Simulation software, the structure is designed using SOLIDWORKS 2022, and its related simulation plug-in simulation can provide relevant static stress analysis module and kinematic simulation motion module. These plug-ins can realize the structure simulation requirements of this paper and have a high integration degree with SOLIDWORKS 2022 design software, which is convenient for the operation of the example.

A. Static stress analysis

The static stress analysis of the structure can be divided into two parts: a. Connecting rod part; b. Slider part.

a. Static stress analysis of connecting rod

This structure plans to grasp an object with a maximum of 3 kg underwater. Considering buoyancy and force Angle and margin, this simulation experiment gives a force of 8N to each of the two vertical contact surfaces in the outer part of the "two fingers" of the "three fingers" structure, and the simulation results are obtained in Fig. 9.

Among them, the place with the largest stress in Fig. 9 (a) is the place where L_2、L_3 is connected, so it can be considered to widen the connection part here and use nuts with higher yield strength. At the same time, the simulation report shows that the safety factor calculated by each nut connection interface is greater than the required safety factor 2. In Fig. 9 (b), it can be seen that the overall displacement is small, and the largest displacement is only 0.2mm.

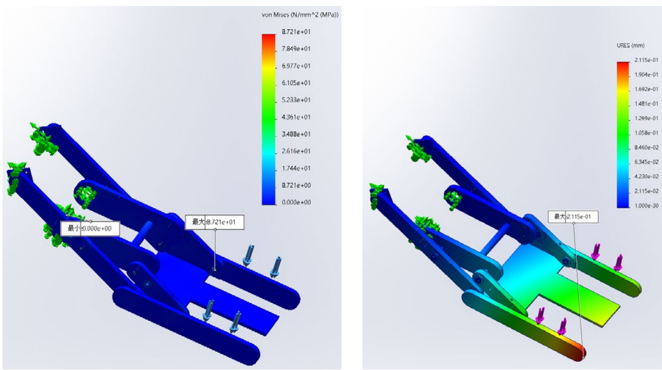

(a) Stress diagram **(b) Displacement diagram**

Fig. 9 The simulation result diagram Ⅰ

In addition, considering that the actual clamping situation may also be a small object, the contact surface is not the "two fingers" outside the "three fingers", but the "fingers" in the middle. Therefore, this experiment also simulates the clamping situation of a small object, and gives a force of 8N to the vertical "one finger" contact surface, and obtains the simulation results in Fig. 10.

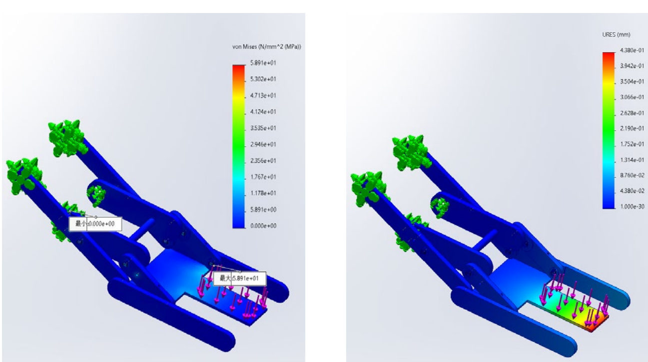

(a) Stress diagram **(b) Displacement diagram**

Fig. 10 The simulation result diagram Ⅱ

Among them, the results of the stress diagram are the same as the last simulation experiment, and the maximum displacement in the displacement diagram is slightly increased, but it is only 0.4mm.

b. Static stress analysis of slider

Because when the mechanical claw grasps the object, the slider slider structure is used as the structure to control the deformation of the mechanical claw, and the slider will cause pressure on the slider when the mechanical claw is stressed. Therefore, it is necessary to analyze the force of the slider to prevent the local deformation of the slider caused by excessive pressure or the loosening of the connection between the parts. Considering a force of 8N at the "three-finger" structure, the slider is given a force of 20N on each side of the direction in Fig. 11 according to the lever theorem.

The figure shows that the maximum stress is at the first bolt fixed connection point between the slider and the upper half of the “Femur” link, and the maximum displacement is only 0.2mm.

Therefore, based on the above simulation results, this paper considers that the structure is sufficient to grasp an object with a maximum weight of 3 kg. The slider and slider structure is made of cast alloy steel, and the other connecting rod parts are made of 1060 aluminum alloy.

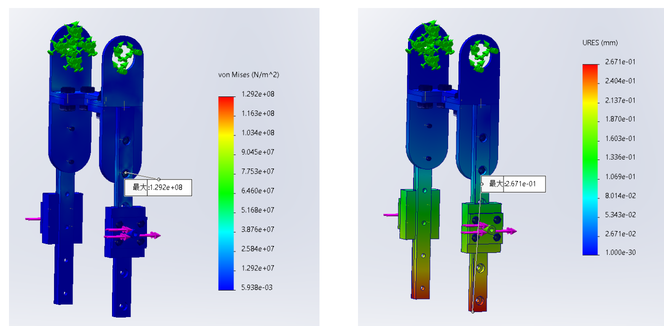

(a) Stress diagram **(b) Displacement diagram**

Fig. 11 The simulation result diagram Ⅲ

B. Kinematic analysis

In order to obtain the appropriate servo specifications, combined with the maximum force selected in the static stress analysis, 8N force was given to the outer and "two fingers" of the "three-finger" structure, and a rotating motor was added to the position of the steering shaft, which was set to rotate one circle in one minute. The movement of five seconds was selected, and the required motor torque of the claw rotating 30° counterclockwise from the starting position was captured, as shown in Fig. 12.

The figure shows that the maximum torque of the required motor is 1317N·mm, which is 13.17Kg·cm. Therefore, this structure needs to select the servo whose maximum torque is greater than this value.

IV. EXPERIMENT AND CHARACTERISTIC EVALUATION

The above is a simulation analysis of the structure proposed in this paper. At the same time, we also completed the manufacturing of the first version of the mechanical leg using 3D printing technology. Fig. 13 is a schematic diagram of its shrinking and opening states. It can be found that, as described earlier in this paper, the grasping end of the mechanical leg obtains a longer grasping range in the open state, and the grasping end of 11cm obtains a grasping space of

17cm. At the same time, the deformation contraction structure of the parallelogram structure also completes the contraction of the grasping end in the limited space. Thus, the contractility of the new mechanical leg designed in this paper can be fully reflected.

After installing mechanical legs on the robot, the team also completed functional verification experiments of grasping two kinds of objects by controlling the steering gear. Fig. 14 is the schematic diagram of the final state of grasping objects of two sizes. Among them, the use of two sides of the baffle and the "three finger" structure of the "middle finger" to complete the grasp of smaller objects; The grasp of larger objects is completed by using two side baffles and "two side fingers" of "three fingers" structure. This reflects the design of the structure of the size of the two sizes of grasping adaptability.

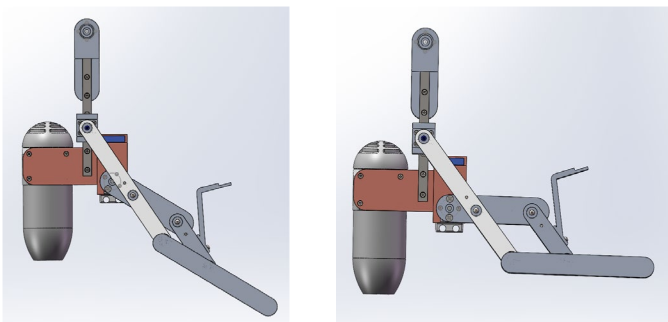

Initial state **Termination state**

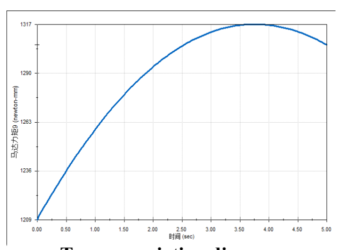

Torque variation diagram

Fig. 12 The simulation result diagram Ⅳ

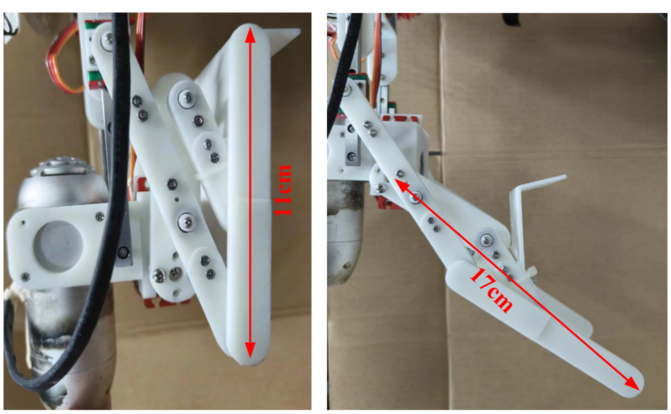

(a) Contraction state **(b) Open state**

Fig. 13 Schematic diagram of the actual mechanical leg: (a) Contraction state; (b) Open state

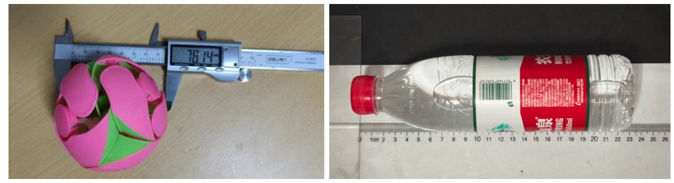

(a) Two objects of smaller and larger size

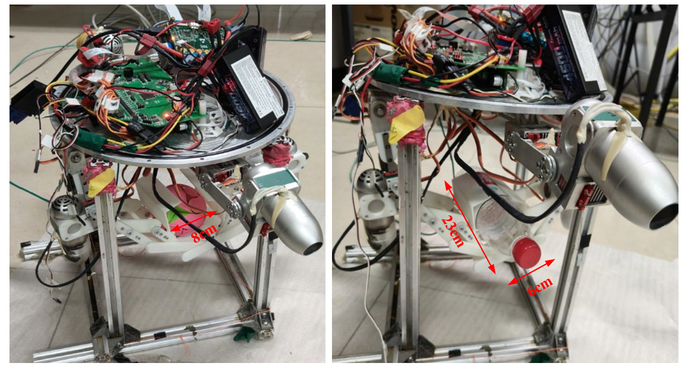

(b) Grab diagram of two objects

Fig. 14 Object grab: (a) Two objects of smaller and larger size; (b) Grab diagram of two objects

V. Conclusion

Based on the above analysis, the simulation results of SOLIDWORKS simulation plug-in can obtain the appropriate specifications and structure size of the steering gear, and verify that the designed structure can have enough structural strength to complete the grasping task of 3kg objects. At the same time, the shrinkage of the structure designed in this paper and the grasping adaptability of the two sizes can be verified by the actual experiment.

It is suggested that this structure can realize the underwater grasping function of a single bionic spherical robot. In the follow-up research, the team will complete the grasping control of the mechanical claw and the motion control of the robot with the object to be grasped on the basis of the object and combined with the actual environment, and finally realize the physical experiment of the robot grasping and moving the object in the water.

References

[1] AJ. Ijspeert, “Amphibious and sprawling locomotion: from biology to robotics and back,” *Annual Review of Control, Robotics, and Autonomous Systems*, vol. 3, pp. 173-193, March 2020.

[2] CY. Li and SX. Guo, “Characteristic evaluation via multi-sensor information fusion strategy for spherical underwater robots,” *Information Fusion*, vol. 95, pp.199-214, July 2023.

[3] K. Ren and JC. Yu, “Research status of bionic amphibious robots: A review,” *Ocean Engineering*, vol. 227, pp. 108862, May 2021.

[4] XJ. Bai, JZ. Shang, ZR. Luo, et al, “Development of amphibious biomimetic robots,” *Journal of Zhejiang University-SCIENCE A*, vol. 23, no. 3, pp. 157-187, March 2022.

[5] RC. An, SX. Guo, L. Zheng, et al, “Uncertain Moving Obstacles Avoiding Method in 3D Arbitrary Path Planning for a Spherical Underwater Robot,” *Robotics and Autonomous Systems*, vol. 151, pp.104011, May 2022.

[6] CY. Li, SX. Guo and J. Guo, “Study on Obstacle Avoidance Strategy Using Multiple Ultrasonic Sensors for Spherical Underwater Robots,”

IEEE Sensors Journal, vol. 22, no. 24, pp. 24458-24470, December 2022.
[7] RC. An, SX. Guo, YH. Yu, et al, “Task Planning and Collaboration of Jellyfish-inspired Multiple Spherical Underwater Robots,” *Journal of Bionic Engineering*, vol. 19, no. 3, pp. 643–656, May 2022.
[8] SX. Guo, S. Cao and J. Guo, “Study on decentralization of spherical amphibious multi-robot control system based on smart contract and blockchain,” *Journal of Bionic Engineering*, vol. 18, no. 6, pp. 1317-1330, December 2021.
[9] H. Yin, SX. Guo and M. Liu, “A virtual linkage-based dual event-triggered formation control strategy for multiple amphibious spherical robots in constrained space with limited communication,” *IEEE Sensors Journal*, vol. 22, no. 13, pp. 13395-13406, July 2022.
[10] B. Liu, HT. Zhang, HF. Meng, et al, “Scanning-chain formation control for multiple unmanned surface vessels to pass through water channels,” *IEEE Transactions on Cybernetics*, vol. 52, no. 3, pp. 1850-1861, March 2020.
[11] YM. Li, JX. Zhang and SC. Tong, “Fuzzy adaptive optimized leader-following formation control for second-order stochastic multiagent systems,” *IEEE Transactions on Industrial Informatics*, vol. 18, no. 9, pp. 6026-6037, September 2021.
[12] SX. Gu, LS. Zhang, SX. Guo, et al, “Communication and Cooperation for Spherical Underwater Robots by Using Acoustic Transmission,” *IEEE/ASME Transactions on Mechatronics*, vol. 28, no. 1, pp.292-301, February 2022.
[13] HL. Dong, JC. Yu, YF. Xu, et al, “MR-GMMapping: Communication efficient multi-robot mapping system via Gaussian mixture model,” *IEEE Robotics and Automation Letters*, vol. 7, no. 2, pp. 3294-3301, April 2022.
[14] J. Hwang and WD. Wang. “Shape Memory Alloy-Based Soft Amphibious Robot Capable of Seal-Inspired Locomotion,” *Advanced Materials Technologies*, vol. 7, no. 6, pp. 2101153, February 2022.
[15] MX. Wu, XX. Xu, Q. Zhao, et al, “A Fully 3D-Printed Tortoise-Inspired Soft Robot with Terrains-Adaptive and Amphibious Landing Capabilities,” *Advanced Materials Technologies*, vol. 7, no. 12, pp. 2200536, June 2022.
[16] JZ. Fan, SQ. Wang, QG. Yu, et al, “Swimming performance of the frog-inspired soft robot,” *Soft robotics*, vol. 7, no. 5, pp. 615-626, October 2020.
[17] R. Baines, SK. Patiballa, J. Booth, et al, “Multi-environment robotic transitions through adaptive morphogenesis,” *Nature*, vol. 610, no. 7931, pp. 283–289, October 2022.
[18] S. Sivčev, J. Coleman, E. Omerdić, et al, “Underwater manipulators: A review,” *Ocean Engineering*, vol. 163, pp. 431-450, September 2018.
[19] JQ. Liu, S. Iacoponi, C. Laschi, et al, “Underwater Mobile Manipulation: A Soft Arm on a Benthic Legged Robot,” *IEEE ROBOTICS & AUTOMATION MAGAZINE*, vol. 27, no. 4, pp.12-26, December 2020.
[20] ZY. Gong, X. Fang, XY. Chen, et al, “A soft manipulator for efficient delicate grasping in shallow water: Modeling, control, and real-world experiments,” *The International Journal of Robotics Research*, vol. 40, no. 1, pp. 449-469, January 2021.
[21] Y. Wang, MX. Cai, S. Wang, et al, “Development and control of an underwater vehicle–manipulator system propelled by flexible flippers for grasping marine organisms,” *IEEE Transactions on Industrial Electronics*, vol. 69, no. 4, pp. 3898-3908, April 2021.
[22] MX. Wu, XW. Zheng, RS. Liu, et al, “Glowing Sucker Octopus (Stauroteuthis syrtensis)-Inspired Soft Robotic Gripper for Underwater Self-Adaptive Grasping and Sensing,” *Advanced Science*, vol. 9, no. 17, pp. 2104382, June 2022.
[23] K. Becker, C. Teeple, N. Charles, et al, “Active entanglement enables stochastic, topological grasping,” *Proceedings of the National Academy of Sciences*, vol. 119, no. 42, pp. 2209819119, October 2022.
[24] CY. Li and SX. Guo, “Adaptive Multi-Mode Switching Strategy for the Spherical Underwater Robot with Hybrid Thruster,” *Advanced Engineering Informatics*, vol. 55, pp. 101845, January 2023.
[25] CY. Li, SX. Guo and J. Guo, “Performance Evaluation of a Hybrid Thruster for Spherical Underwater Robots,” *IEEE Transactions on Instrumentation & Measurement*, vol. 71, pp.1-10, June 2022.
[26] CY. Li and SX. Guo, “Performance Evaluation of Spherical Underwater Robot with Attitude Controller,” *Ocean Engineering*, vol. 268, pp. 113434, January 2022.